Closing the Gap between the Workshop and Numerical Simulations in Sheet Metal Forming

B.D.Carleer[1] and **J.Huétink**[1]

Abstract. The accuracy and reliability of numerical simulations of sheet metal forming processes do not yet satisfy the industrial requirements. In this paper we pay attention to the strategies which can be followed to decrease the gap between the real deepdrawing process and the predictions obtained from the simulation. We will focus on three aspects to improve the numerical simulations. The contact search for an accurate contact and friction behaviour is treated firstly. The friction behaviour itself is the second point of attention. Thirdly, attention is paid to drawbead modelling in 3D simulations.[1]

1. INTRODUCTION

Numerical simulation capabilities of sheet metal forming processes are currently at a stage where simulations can be applied as a useful tool in solving industrial problems. However, the accuracy of predictions obtained from a simulation are not obvious. Industry requires that simulation programs serve as a reliable design tool and hence these programs must be robust and accurate. The gap between the industrial requirement and the current state of numerical simulation capabilities is due to limitations of numerical procedures as well as a lack of knowledge of the physics.

Limitations of the numerical procedures are:

- The refinement of the discretisation and the required cpu time; details like drawbeads cannot be modelled in a full scale 3D simulation without increasing the cpu time considerably.
- The interface between the design, CAD, packages and the simulation code; FEM-meshes which can be obtained from CAD-packages cannot satisfy the requirement for fast contact algorithms used in the simulation code.
- The solution algorithm; the application of explicit solutions versus implicit. In most sheet metal forming processes inertia effects can be neglected. Hence it seems rather artificial to apply unrealistic velocities and accelerations only because of the dynamic explicit code.

Limitations in knowledge of physics are:

- The lack of accuracy of constitutive equations, particularly in the high deformation range.
- The lack of accuracy of the description of friction and lubrication between tool and blank.

In this paper attention is paid to the strategies which can be followed to decrease the gap between the real deepdrawing process and the predictions obtained from the simulation. In the deepdrawing process a blank is deformed by a number of tools. The blank is clamped between the blankholder and the die. The punch pushes the blank into the desired shape. This interaction between the tools and the blank is very important. So in deepdrawing simulations this is also a major field of interest.

2. CONTACT SEARCH

It is important to know where the tool and the blank make contact. The contact search must be accurate and fast. The tools are, most of the time, designed with the help of CAD-packages. The tool geometry is described with several surfaces. For finite element simulations these surfaces are meshed to obtain a proper tool description. Due to tolerances in the CAD-packages the surfaces are not adjacent. The mesher creates large elements for flat areas and small elements where small radii occur. The result is a minimum of elements for a proper tool description. The advantage of a small number of elements is a fast contact search. A disadvantage of this meshing method is the non-adjacent elements.

Figure 1 shows an example of a tool meshed by a CAD-package. At the transition from the flat area to the radius the elements are not adjacent and there is also a change form large elements to small elements. The size and the aspect ratio of the tool elements can be very different because of the separate meshing of the surfaces. The contact search must handle the lack of connectivity and the strongly differing aspect ratios.

[1] University of Twente, Department of Mechanical Engineering, P.O.Box 217, 7500 AE Enschede

ECCOMAS 96
Published in 1996 by John Wiley & Sons, Ltd

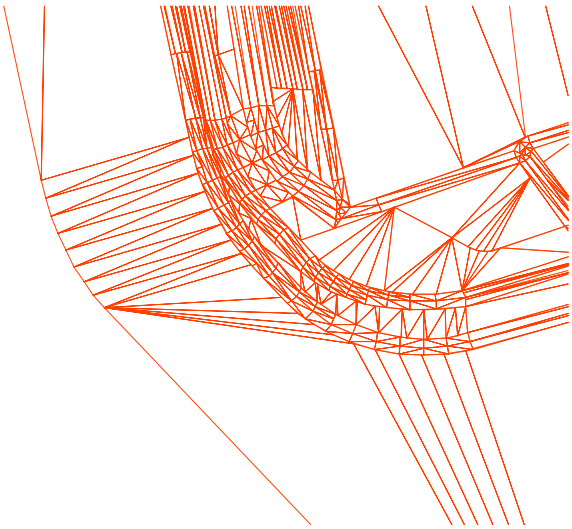

Figure 1. Example of a detail of a product meshed by a CAD-package

The contact search is split into two steps. First, a global search is performed which delivers a number of tool elements where the contact can take place. Second, a local search is done to find the exact place of contact. The global search must handle the problem of non adjacent elements and the varying element size. Here a global search has been developed based on the pinball algorithm introduced by Belytschko (see [1] and [2]) for contact-impact problems.

2.1 Pinball search

The new developed contact search algorithm uses the pinball algorithm. Around all tool elements as well as around all blank nodes imaginary spheres are created. These spheres are designated as pinballs. The principle of the global search is to check the distance between the centres of the pinball of a blank node and the tool pinballs, see figure 2.

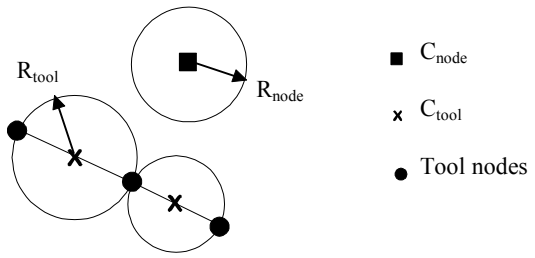

Figure 2. Principle of the pinball search with the pinballs of the tool and the pinball of the blank node

If penetration of these pinballs occurs, the element belonging to the tool pinball is further taken into account for the local search. Penetration is noticed when the distance between the centre of the blank node pinball, C_{node}, and the centre of the tool pinball, C_{tool}, is smaller than the sum R of the radii of these pinballs. In formula this can be written as:

$$\left\| C_{node} - C_{tool} \right\| < R \qquad (1)$$

Where $\| \ \|$ denotes the Euclidean vector norm. After having checked all necessary tool pinballs a set of elements where contact with the blank node can occur is obtained. With these elements the local searches are executed. If no penetration with any tool pinball is found, no contact occurs. The global search is very fast because there is only a comparison of co-ordinates. An important parameter for a well functioning contact algorithm is probably the pinball size. It may not be too large because then the global search is more often successful than necessary. Either, it may not be to small. In that case the danger exists of observing contact too late. In contrast to Belytschko's method the pinball size will vary during the simulation.

Firstly, the tool pinball is considered. The tool pinball radius exists of a constant value and a variable value, equation (2). The constant value depends on the element size. The centre of the pinball and the pinball radius are constructed in such a way that the pinball radius is as small as possible. But the sphere must contain the whole element. When the pinball radius becomes too large, the element can be split in more than one pinball. The constant value is denoted as R_0. The variable value of the radius depends on the displacement of the tool. This pinball enlargement is necessary because otherwise possible contact will be missed if the tool displacement is large compared to the pinball size.

$$R_{tool} = R_0 + \Delta U_{tool} \qquad (2)$$

Secondly, the node pinball is considered. For the node pinball, two phases can be distinguished. In the first phase, the pre-contact phase, the node is not in contact with the tool. During this phase the radius is set at a start value, R_S. This minimum radius of the blank pinballs has to be enlarged with the nodal displacement to prevent missing contact during large displacements. In the second phase, the post-contact phase, the node is in contact. During this phase the radii of the node pinballs are set to the nodal displacement increased with the penetration in the tool. The node can penetrate the tool elements because of the penalty method used in the contact algorithm. The node pinball radius is set:

$$R_{node} = R_S + \Delta U_{node} \quad : pre - contact \qquad (3)$$
$$= \Delta U_{node} + gap : post - contact$$

The global search selects a number of elements for the local search. The local search is an orthogonal projection on the selected elements. The shortest projection is the position where the blank node makes contact with the tool.

The algorithm is demonstrated with a deep drawing simulation of a square cup. The punch, the blankholder and the die are modelled with the aid of a number of surfaces. The result is a tool description with non-adjacent elements and varying element sizes. Due to the symmetry only one quarter of the tools were modelled. The tool meshes are shown in figure 3.

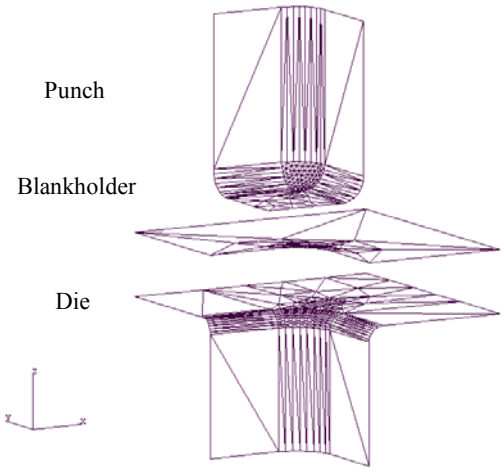

Figure 3. Element mesh of the tool for the square cup deep drawing simulation

The search algorithm can deal with the non-adjacent elements and the varying element size in a time effective way. The following figure shows the deformed mesh of the square cup.

It is important for a finite element code to handle with this kind of tool descriptions. The contact search enables a fast interface with CAD-packages. In the pre-processing phase the surfaces must not be smoothed or joined manually anymore. This results in a considerable saving of time.

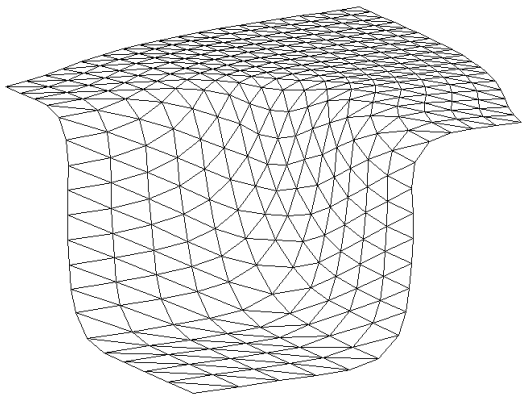

Figure 4. Deformed blank of the square product.

3. FRICTION MODEL

When the blank and the tool are in contact they do not penetrate and they can slide along each other. In order to describe sliding an often used friction model is the Coulomb model in which the coefficient of friction, 💻, is an overall constant parameter.

$$F_f = \mu F_n \qquad (4)$$

Where F_f is the friction force and F_n is the normal force. From a tribological point of view this constant value of μ is not satisfying because it depends on local contact conditions. According to Schey (see [7])there are several different contacts between the sheet and the tools for each sheet metal forming process. Therefore a good friction model needs a coefficient of friction which depends on the local contact conditions.

In the work of Schipper (see [8]) the coefficient of friction is presented as a function of the dimensionless lubrication number L:

$$L = \frac{\eta \cdot v}{p \cdot R_a} \qquad (5)$$

With:
- η : the dynamic lubricant viscosity
- v : the sum velocity of the contact surfaces
- p : the mean contact pressure
- R_a : the CLA surface roughness

When the coefficient of friction is plotted as a function of the lubrication number the following graph is found, figure 5.

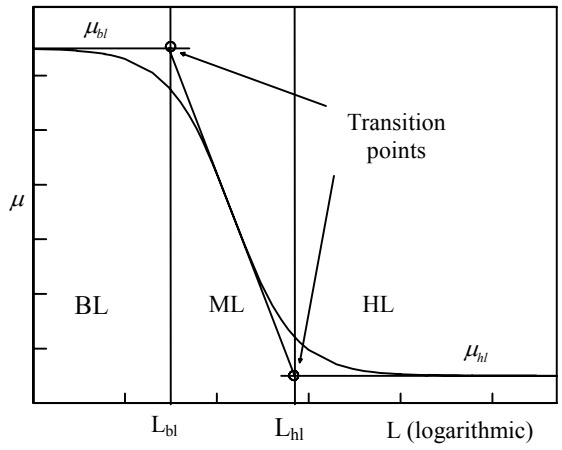

Figure 5. Generalised Stribeck curve

In this figure, the generalised 'Stribeck' curve, three different zones can be distinguished. On the left hand side of the graph μ has a constant high value. This is the boundary lubrication regime, BL. Under these conditions the load on a contact is completely carried by the interacting surface asperities. On the right hand side the value of μ is rather low. Under these conditions the load on the contact is fully carried by the lubricant. The lubricant separates the surfaces totally. This is called the hydrodynamic lubrication regime, HL. The region in between is called the mixed lubrication regime, ML. The load is partly carried by the surface asperities and partly by the pressurised lubricant.

According to the operational condition contact μ can have a varying value during the process. The use of a model which describes the frictional behaviour in this way would be a large improvement for the simulations. It is possible to use a mathematical formula, obtained by curve fitting techniques, for the desired dependency of μ on the operational condition.A suitable curve fit is defined by the following equation (see [4]):

$$\mu(L) = \frac{1}{2}\left(\left(\mu_{bl} + \mu_{hl}\right) + \left(\mu_{bl} - \mu_{hl}\right) \tanh\left(\frac{\log\left(\frac{L^2}{L_{bl} \cdot L_{hl}} \right)}{\log\left(\frac{L_{bl}}{L_{hl}} \right)} \right) \right) \quad \textbf{(6)}$$

With: μ_{bl} : BL value of μ

μ_{hll} : HL value of μ

L_{bl} : L at BL to ML transition

L_{hl} : L at ML to HL transition

With this expression the value of μ has become dependent on the local contact conditions as they are present in each single contact area. This curve fit has been implemented and used as a pragmatic friction model.

As the determination of the transition points is necessary, experimental date representative for sheet metal forming has to be available. For this reason experiments were carried out on a testing device which was especially designed for contacts operating under sheet metal forming conditions.

The effect of the more physically based friction model is shown by a simulation of the deepdrawing of a square. Four simulations were performed. One with a constant friction coefficient of 0.144 and three with the Stribeck friction model. With the Stribeck friction model three different punch velocities were used, 1 mm/s, 10 mm/s and 100 mm/s.

In figure 6 the punch force for deepdrawing of a quarter of the square cup for the four simulations are presented. The constant friction and the Stribeck friction for 1 mm/s gave the same punch force. When the punch velocity is increased to 10 mm/s or to 100 mm/s the punch force decreases. This is caused by the fact that more and more contacts start to operate in the ML regime instead of in the BL regime. It can be seen that the punch force decreases from 14.6 kN for constant friction to 12.0 kN for Stribeck friction with a punch velocity of 100 mm/s

When the strains and the stresses of the blank were compared, also some differences were found. Especially material which was originally under the blankholder shows different results. The sliding velocity in that area increases with increasing punch speeds. Due to the increasing velocity the friction force decreases and the material flows easier into the die. This results in a different strain distribution in the blank.

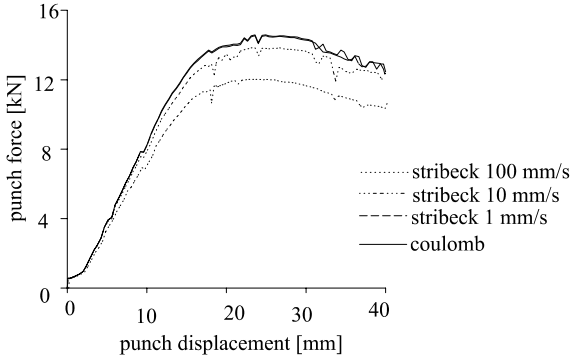

Figure 6. Punch force versus punch displacement for four simulations.

4. DRAWBEAD MODEL

In order to control the flow of the material drawbeads are used. In finite element simulations the drawbead geometries are seldom included because of the small radii. A very large number of elements is required to model small radii in 3D simulations. For economic reasons an equivalent drawbead model has been developed. The characteristics of this equivalent drawbead model are obtained from a local (2D plane strain) simulation or from experimental data.

4.1 2D Drawbead Model

To obtain more insight in the drawbead behaviour a 2D analysis was performed. This analysis gave information on the drawbead restraining force and the strain changes in the blank (see [3]).

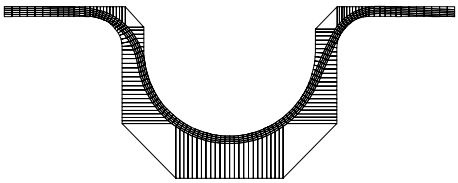

Figure 7. Finite element mesh for the 2D analysis of the drawbead.

The sheet was modelled with four layers of four node plane strain elements (figure 7). The contact elements are also depicted in this figure. The total number of elements for the sheet was 400. In the simulation, the mixed Eulerian-Lagrangian formulation was used. The mesh is fixed in flow direction and perpendicular to the flow the mesh is free to move. The advantage of this formulation is that the grid refinements remain at their place and the effects of sheet thinning can be described. The resistance of the sheet to move through the drawbead is caused by friction and by bending and unbending of the sheet.

In figure 8 the calculated force to pull the sheet through the drawbead and the tangential strain of the sheet are printed. Both characteristics as a function of the sheet displacement. The tangential co-ordinate lies in the profile direction of the sheet. Since a plane strain state is assumed and the material is modelled to be almost incompressible, the thickness strain has the same value (except for the sign) as the tangential strain.

At Hoogovens Research & Development experiments were performed for verification of this 2D model. Comparing the thickness distribution the measured and the calculated values agreed very well. Also the forces compared well. So, the 2D model is an accurate model to gain information about the drawbead behaviour.

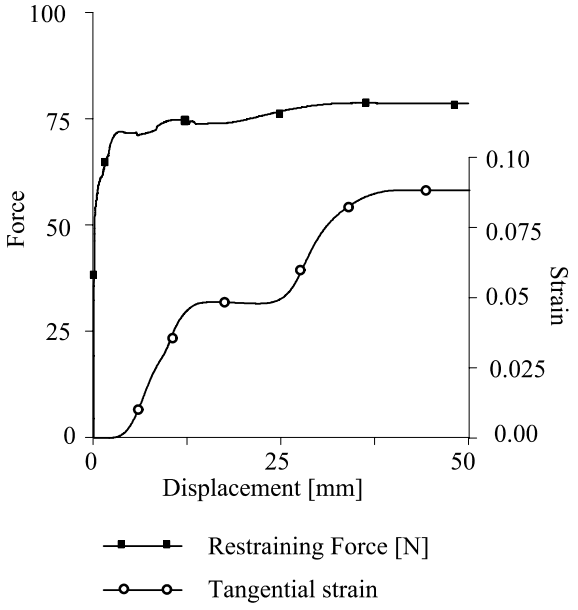

Figure 8. Numerical results of the 2D analysis of the drawbead.

4.2 Equivalent drawbead

The equivalent drawbead is defined as a line on the tool surface. If an element passes the equivalent drawbead line a restraining force acts on that element. But this restraining force is not enough to describe the whole drawbead behaviour. So, besides a restraining force also an additional thickness strain should be added to the element (see [6]).

The restraining force acts normal to the drawbead line opposite to the material flow. This force is taken into account at the right hand side of the finite element equations as a body force.

$$\underline{K} \cdot \Delta\underline{u} = \Delta\underline{F} + \underline{F}_{db} \qquad (7)$$

With: $\underline{K}$: Stiffness matrix
$\Delta\underline{u}$: displacement increment
$\Delta\underline{F}$: force increment
$\underline{F}_{db}$: restraining force

The restraining force is calculated by integrating the drawbead force per unit width over the length of the

elements which crosses the drawbead line:

$$\underline{F}_{db} = \int_{l} f_{db}\, dl \qquad (8)$$

The restraining force is history dependent. Its value is a function of the material displacement through the drawbead. The added force is a curve fit form the drawbead force per unit width, which in turn is obtained from the 2D analysis.

The implementation of the drawbead strain needs more attention. The strain is also history dependent and obtained form the 2D drawbead analysis. To implement the additional strain it is stated that the drawbead gives an extra stiffness. In this case the finite element equation looks as follows:

$$\left(\underline{K} + \underline{K}_{db}\right) \cdot \Delta\underline{u} = \Delta\underline{F} \qquad (9)$$

Where $\underline{K}_{db}$ is the drawbead stiffness matrix. This equation can be reordered:

$$\underline{K} \cdot \Delta\underline{u} = \Delta\underline{F} - \underline{K}_{db} \cdot \Delta\underline{u} \qquad (10)$$

The drawbead stiffness term can be rewritten in drawbead stresses:

$$\underline{K} \cdot \Delta\underline{u} = \Delta\underline{F} - \int_{V} \underline{B}^{T} \cdot \underline{\sigma}_{db}\, dV \qquad (11)$$

The only thing that must be done is an estimation of the drawbead stresses $\underline{\sigma}_{db}$. These stresses can be calculated out of the prescribed drawbead strains.

Summarising, the equivalent drawbead model exists of two components (figure 9). First, the prescribed force which restrains the element of sliding too fast through the drawbead. Second, the prescribed strain which elongates the element. In this way the element becomes thinner. These two components are added up to give the complete drawbead describtion.

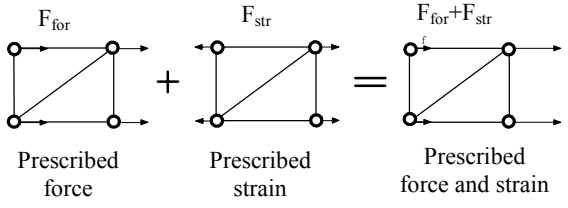

Figure 9. Summary of the equivalent drawbead model.

A strip drawing simulation is performed to show the working of the equivalent drawbead model. The geometry of the tools is identical to the tools of the square cup. Now only a strip is drawn instead of a whole blank. The equivalent drawbead is defined as a line in the die/blankholder region. The drawbead force and drawbead strain are both history dependent. Two simulations are performed. In the first simulation only the drawbead restraining force is applied. In the second simulation both the restraining force and the drawbead strain are included. In figure 10 the deformed mesh as well as the thickness strain distribution of both simulations are shown. At the deformed mesh the co-ordinate distance is indicated starting at the line of symmetry under the punch, 0.0 mm. The punch radius is situated at a co-ordinate distance of 35.0 mm, the die radius at 75.0 mm and the end of the strip at a distance of 104 mm.

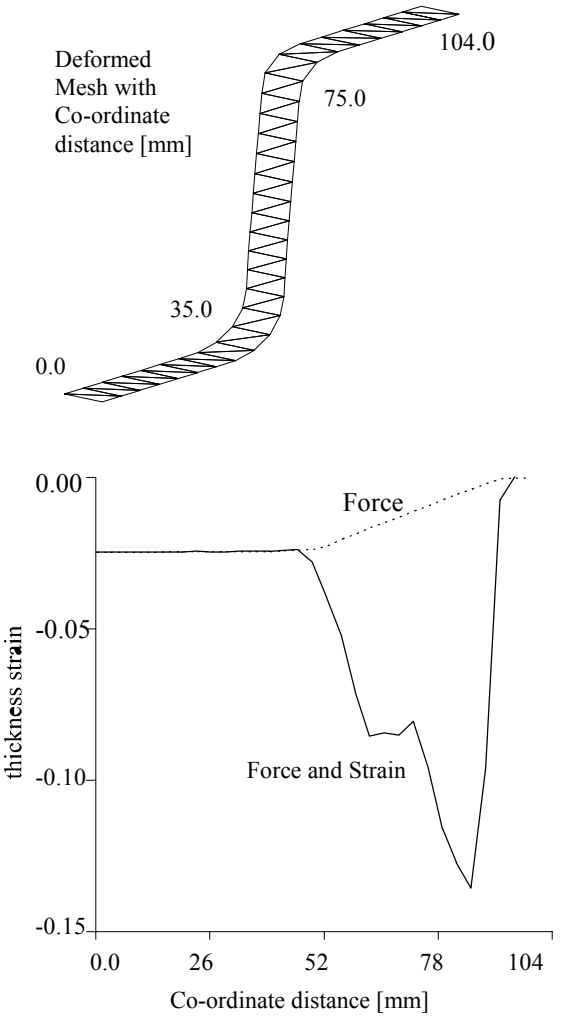

Figure 10. Thickness strain distribution of the strip drawing simulation

The thickness strain for the simulation with the restraining force is -0.025 for the material under the punch (co-ordinate distance form 0 to 35). The simulation with both the restraining force and the thickness strain shows the same strain distribution under the punch. But for this simulation the strain in the rest of the strip is much larger. At co-ordinate distance 65 a plateau of -0.08 can be seen. A peek of -0.13 is seen at distance 90. This is just after the drawbead line. The characteristic of the strain distribution is like the strain characteristic of the 2D model (figure 8). It must be mentioned that for this drawing simulation not the strain curve of figure 8 is used.

This latter simulation shows a strain distribution which is similar to the strain distribution found in the experiments. Modelling drawbeads by only applying an additional restraining force does not incorporate the modified material properties. For this reason the equivalent drawbead must incorporate the effect of sheet thinning and the change of the strain distribution.

5. CONCLUDING REMARKS

Now we have a complete description of the blank tool interaction which is the driving force for forming the sheet. The contact search algorithm can handle the non adjacent tool description gained from CAD-packages. The friction behaviour based on local contact conditions gives a more complete friction model. Even drawbeads can be incorporated in a time effective and efficient way.

Parallel to the developments of the numerical procedures an experimental program has begun. This program focuses on the development of constitutive equations and on the friction/lubrication behaviour has begun.

6. ACKNOWLEDGEMENTS

The authors thank Hoogovens Research & Development for performing the drawbead experiments and their support in this research.

REFERENCES

[1] T.Belytschko and M.O.Neal, *Contact-impact by the pinball algorithm with penalty and Lagrangian methods*, 547-572, Int. J. Num. Meth. Eng., 31, 1991

[2] T.Belytschko and I.S. Yeh, *The splitting pinball method for contact-impact problems*, 375-393, Comp. Meth. Appl. Mech. Eng., 105, 1993

[3] B.D. Carleer, P.T. Vreede, M.F.M. Louwes, J. Huétink, *Modelling Drawbeads with Finite Elements and Verification*, 63-68, J. Mat. Proc. Tech., Vol 45/1-4 1994

[4] R. ter Haar, *Friction in Sheet Metal Forming, the influence of (local) contact conditions and deformation*, PhD dissertation, University of Twente, 1996

[5] M.D,P. Kerkhoff, *A Modified Pinball Contact Algorithm for Deep Drawing Simulations based on CAD Data*, Graduate report, University of Twente, 1995

[6] V.T. Meinders, *Drawbead Modelling in 3D Deep Drawing Processes*, Graduate report, University of Twente, 1996

[7] J.A. Schey, *Tribology in Metalworking, Friction< Lubrication and Wear*, ASM, Metals Park, Ohio, USA, 1983

[8] D.J. Schipper, *Transition in the lubrication of concentrated contacts*, PhD dissertation, University of Twente, 1988